Published OnlineFirst September 23, 2020; DOI: 10.1158/1535-7163.MCT-20-0116

Preclinical Development of MGC018, a Duocarmycin-based Antibody–drug Conjugate Targeting B7-H3 for Solid Cancer

Juniper A. Scribner[1], Jennifer G. Brown[2], Thomas Son[1], Michael Chiechi[1], Pam Li[1], Sharad Sharma[2], Hua Li[2], Anushka De Costa[1], Ying Li[1], Yan Chen[1], Ann Easton[1], Nicholas C. Yee-Toy[1], Francine Z. Chen[1], Sergey Gorlatov[2], Bhaswati Barat[2], Ling Huang[2], Christina R. Wolff[2], Jeff Hooley[1], Tim E. Hotaling[1], Timur Gaynutdinov[2], Valentina Ciccarone[2], James Tamura[2], Scott Koenig[2], Paul A. Moore[2], Ezio Bonvini[2], and Deryk Loo[1]

ABSTRACT

B7-H3, also referred to as CD276, is a member of the B7 family of immune regulatory proteins. B7-H3 is overexpressed on many solid cancers, including prostate cancer, renal cell carcinoma, melanoma, squamous cell carcinoma of the head and neck, non–small cell lung cancer, and breast cancer. Overexpression of B7-H3 is associated with disease severity, risk of recurrence and reduced survival. In this article, we report the preclinical development of MGC018, an antibody–drug conjugate targeted against B7-H3. MGC018 is comprised of the cleavable linker-duocarmycin payload, valine-citrulline-*seco* duocarmycin hydroxybenzamide azaindole (vc-*seco*-DUBA), conjugated to an anti-B7-H3 humanized IgG1/kappa mAb through reduced interchain disulfides, with an average drug-to-antibody ratio of approximately 2.7. MGC018 exhibited cytotoxicity toward B7-H3–positive human tumor cell lines, and exhibited bystander killing of target-negative tumor cells when cocultured with B7-H3–positive tumor cells. MGC018 displayed potent antitumor activity in preclinical tumor models of breast, ovarian, and lung cancer, as well as melanoma. In addition, antitumor activity was observed toward patient-derived xenograft models of breast, prostate, and head and neck cancer displaying heterogeneous expression of B7-H3. Importantly, MGC018 exhibited a favorable pharmacokinetic and safety profile in cynomolgus monkeys following repeat-dose administration. The antitumor activity observed preclinically with MGC018, together with the positive safety profile, provides evidence of a potentially favorable therapeutic index and supports the continued development of MGC018 for the treatment of solid cancers.

Graphical Abstract: http://mct.aacrjournals.org/content/molcanther/19/11/2235/F1.large.jpg.

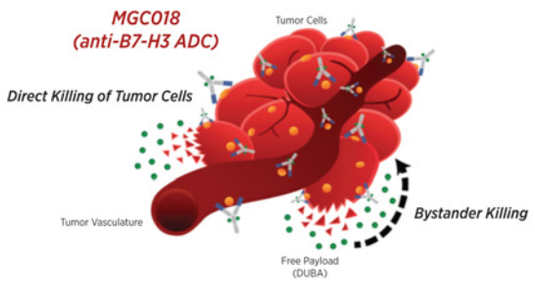

MGC018 ADC targets B7-H3 on tumor cells and tumor-associated vasculature and mediates bystander killing

Introduction

B7-H3, also referred to as CD276, is a member of the B7 family of immune regulatory proteins (1). B7-H3 is a type-1 transmembrane glycoprotein containing extracellular immunoglobulin-like domains. Two species-specific isoforms of B7-H3 have been reported. Mice display a 2-Ig B7-H3 form, while the primate counterpart has undergone gene duplication and is expressed as a 4-Ig–containing molecule (2, 3). Although a specific receptor or receptors that bind B7-H3 have not been identified conclusively, B7-H3 has been implicated experimentally in the delivery of both costimulatory and inhibitory signals (1, 4). Most published data, however, demonstrate an inhibitory role for B7-H3 in immune responses (5), including *in vitro* studies examining T-cell responses (2, 6), mouse knockout (KO) studies (7, 8) and structure/function analyses based on the B7-H3 crystallography data (9, 10), and supports the hypothesis that B7-H3 has a role in evading antitumor immunity.

B7-H3 is overexpressed on many cancers, including, but not limited to, prostate cancer (11–14), melanoma (13, 15), breast cancer (13, 16, 17), non–small cell lung cancer (13, 18, 19), and oral squamous carcinoma (20). In renal cell carcinoma, B7-H3 is broadly expressed by both the tumor epithelium and tumor-associated vasculature (13, 21). In many cancers, overexpression of B7-H3 has been correlated with multiple adverse clinical and pathologic features of disease, increased risk of recurrence, and reduced survival. Conversely, although B7-H3 mRNA expression is detectable in most normal tissues, B7-H3 protein expression is limited in normal tissues (13, 22, 23).

[1]MacroGenics, Inc., Brisbane, California. [2]MacroGenics, Inc., Rockville, Maryland.

Note: Supplementary data for this article are available at Molecular Cancer Therapeutics Online (http://mct.aacrjournals.org/).

Corresponding Author: Deryk Loo, MacroGenics, Inc., 3280 Bayshore Blvd., Suite 200, Brisbane, CA 94005. Phone: 650-624-2736; Fax: 650-624-2793; E-mail: lood@macrogenics.com

Mol Cancer Ther 2020;19:2235–44

doi: 10.1158/1535-7163.MCT-20-0116

©2020 American Association for Cancer Research.

Downloaded from mct.aacrjournals.org on February 1, 2021. © 2020 American Association for Cancer Research.

Published OnlineFirst September 23, 2020; DOI: 10.1158/1535-7163.MCT-20-0116

Notwithstanding its negative prognostic association in cancer, the biological role of B7-H3 remains unclear and controversial, a difficulty compounded by the lack of a known B7-H3 receptor. Accordingly, we have sought to develop antibody-based targeting agents that exploit the overexpression of B7-H3 by tumors. Enoblituzumab (MGA271) is an anti-B7-H3 mAb bearing an engineered Fc domain optimized to enhance antitumor effector-mediated function (13), while MGD009 is a CD3 × B7-H3 DART® molecule designed to recruit the cytolytic activity of T-cell killing toward B7-H3–positive tumors.

Antibody–drug conjugates (ADC) combine the target specificity of a mAb with cytotoxic agents, with the goal of delivering the cytotoxic agent to the tumor and improving the therapeutic index. Advances over the past couple of decades has led to development of linkers with greater serum stability and payloads with greater potency and various mechanisms of action. These advances have contributed to the approval of 9 ADCs for the treatment of cancer. The improvements in ADC technologies and clinical successes prompted us to investigate whether overexpression of B7-H3 in cancer provides an opportunity for targeted therapy with an ADC, which may complement and/or enhance B7-H3 targeting by immune-based agents.

Here, we report the preclinical development of MGC018, a duocarmycin-based humanized ADC targeting B7-H3. MGC018 exhibited cytotoxicity toward B7-H3–positive human tumor cell lines, including bystander killing, potent antitumor activity in preclinical tumor models, and a favorable pharmacokinetic and safety profile in cynomolgus monkeys.

Materials and Methods

Humanization

To construct the humanized anti-B7-H3 mAb MGA017, humanized PRCA157 variable light chain (VL) and PRCA157 variable heavy chain (VH) amino acid sequences (Supplementary Fig. S1) were designed using the complementary-determining region (CDR) sequences from the mouse PRCA157 mAb and framework sequences from human germline V-kappa or VH segment, respectively. The humanized PRCA157 VL and VH coding sequences were synthesized *de novo*, and fused to the human C-kappa or human gamma 1 constant region cDNA, respectively.

Conjugation to vc-*seco*-DUBA and hydrophobic interaction chromatography purification

Conjugation of humanized anti-B7-H3 mAb (MGA017) to vc-*seco*-duocarmycin-hydroxybenzamide azaindole (DUBA), and hydrophobic interaction chromatography (HIC) to enrich for DAR2 and DAR4 species, was performed by Byondis B.V. as described previously (24). A schematic representation of the MGC018 ADC structure is shown in Supplementary Fig. S2. Drug distribution and drug-to-antibody ratio (DAR) average by HIC for MGC018 is shown in Supplementary Fig. S3. An anti-CD20 mAb conjugated to vc-*seco*-DUBA was employed as a control ADC. Analytic characteristics of MGC018 are summarized in Supplementary Table S1.

Tumor cell line culture

MDA-MB-468, A375.S2, PA-1, Calu-6, Hs700T, SW48, and LN-229 tumor cell lines were obtained from ATCC and cultured in DMEM/F-12 media containing 10% FBS. NCI-H1703 and Raji tumor cell lines were obtained from ATCC and cultured in RPMI1640 media containing 10% FBS. Quantitative determination of cell surface antigen by quantitative flow cytometry (QFACS) is described in the Supplementary Materials and Methods. All cell lines were thawed from working cell banks, which were screened for *Mycoplasma* by PCR. Cell line identity was confirmed by short tandem repeat profiling at ATCC, and studies were performed with cultures that had undergone fewer than 25 passages.

Generation of Hs700T/B7-H3 KO tumor cell line

The Hs700T/B7-H3 KO line was generated using transEDIT clustered regularly interspaced short palindromic repeats (CRISPR) gRNA huCD276, pCLIP-All-EFS-Puro (TEVH-1194322) according to the manufacturer's protocol (transOMIC Technologies). Details on generation of the KO line and flow cytometry analysis is described in the Supplementary Materials and Methods.

Cytotoxicity assays

Cells were harvested by trypsinization and plated at 5,000 cells/well with serially diluted MGC018 then incubated at 37°C. Viability was measured after 7 days using alamarBlue according to manufacturer's protocol (Thermo Fisher Scientific). Plates were read on a SpectraMax Gemini (Molecular Devices). Data were analyzed using GraphPad Prism (4-parameter curve fit analysis; v7.02, GraphPad) to determine IC_{50} (half-maximal inhibitory concentration) values.

Bystander killing assay

Hs700T/B7-H3 KO cells stably expressing red fluorescent protein (Hs700T/B7-H3 KO/RFP) were generated using the IncuCyte NucLight Red Lentivirus (Sartorius) according to manufacturer's protocol. Cells were harvested by trypsinization and plated into 96-well flat bottom plates. Parental Hs700T cells were plated at densities ranging from 0 to 5,000 cells/well. Hs700T/B7-H3 KO/RFP cells were plated at 5,000 cells/well. MGC018 was added to plates at the indicated concentrations, then plates were incubated at 37°C and cell viability of Hs700T/B7-H3 KO/RFP cells was measured after 5 days using an IncuCyte Live-Cell Analysis System (Sartorius).

In vivo efficacy

Efficacy studies were carried out under protocols approved by MacroGenics, Inc. Institutional Animal Care and Use Committee.

Female CD-1 nude (homozygous) mice (Crl:CD1-*Foxn1*^{nu}) and female SCID/CES1c KO mice (5–7 weeks old) were obtained from Charles River Laboratories and maintained under pathogen-free conditions, with food and water supplied ad libitum. Human tumor cells (5×10^6) were resuspended in 1:1 medium (DMEM/F-12) and Matrigel basement membrane matrix (Corning) and implanted subcutaneously into the flank (A375.S2, Calu-6, PA-1) or mammary fat pad (MDA-MB-468) of mice. Mice were randomized into groups of 5-7 individuals per group. ADCs or vehicle control (PBS) were administered intravenously by tail vein injection (10 mL/kg) following growth of established tumors (100–150 mm^3). Tumors were measured twice weekly by orthogonal measurements with electronic calipers, with tumor volumes calculated as: (length × width × height)/2. Details on statistical analyses are provided in the Supplementary Materials and Methods.

Patient-derived xenograft (PDX) studies were performed at Champions Oncology. Female Athymic Nude-*Foxn1*^{nu} from Envigo (head and neck, triple-negative breast cancer models) or male NOG mice from Taconic (prostate cancer model), 6–8 weeks of age, were used for the PDX studies. Low passage tumor fragments were implanted into stock animals. When tumors reached 1.0–1.5 cm^3, they were reimplanted into prestudy animals unilaterally on the left flank. When tumors reached an average tumor volume of 150–300 mm^3, animals were matched by tumor volume into treatment or vehicle control

Downloaded from mct.aacrjournals.org on February 1, 2021. © 2020 American Association for Cancer Research.

Published OnlineFirst September 23, 2020; DOI: 10.1158/1535-7163.MCT-20-0116

groups. Three animals were assigned to each group and dosed intravenously by tail vein injection (10 mL/kg). Tumor volumes were measured twice weekly by calipers. Tumor volume was calculated using the formula TV = (width × 2) × length × 0.52. The study endpoint was determined when the mean tumor volume of the control group reached 1,500 mm^3 up to a maximum day of 60.

In vitro serum stability and *in vivo* pharmacokinetics

Methods assessing *in vitro* serum stability and *in vivo* pharmacokinetics in mice and cynomolgus monkeys are described in the Supplementary Materials and Methods.

Toxicology

A repeat-dose toxicology study was conducted in naïve cynomolgus monkeys. Treatment groups (5 male/5 female) were administered either the control article (0.9% sodium chloride for injection USP) or MGC018 every 3 weeks (1, 3, 6, or 10 mg/kg/dose), for a total of three doses, by intravenous infusion over 1 hour. Six animals per group (3/sex/group) were necropsied on day 57, while the remaining recovery group animals (2/sex/group) were necropsied on day 120 following an 11-week recovery period. Mortality, clinical signs, body weights, food consumption, clinical pathology, and toxicokinetics were monitored prior to and throughout the study. Indirect ophthalmoscopy was performed prestudy and prior to terminal sacrifice by a veterinary ophthalmologist. Following terminal sacrifice, gross necropsy, measurement of organ weights, and histopathologic examinations were conducted.

Results

Selection and generation of MGC018

A pool of anti-B7-H3 mAbs was generated from a series of intact cell immunizations (13). The anti-B7-H3 mAb PRCA157 was selected as an ADC candidate from the pool of anti-B7-H3 mAbs based on its characteristics, including affinity, tumor versus normal tissue cross-reactivity profile, cynomolgus monkey B7-H3 cross-reactivity, cell internalization, and antitumor activity from screens as monomethyl auristatin E–based ADCs (25). PRCA157 was humanized by CDR grafting and fused to human C-kappa and gamma 1 constant regions, yielding the precursor MGA017 mAb, which retained the B7-H3 binding affinity of the parental murine mAb. When selecting a linker-payload, it is important to consider the target biology to maximize potential antitumor activity and safety. B7-H3 is expressed heterogeneously within the tumor epithelium of solid cancers, and is also expressed by tumor-associated vasculature (21, 26) and cancer stem-like cells (27), therefore a linker-payload that possessed bystander killing activity and the ability to kill slow-dividing or nondividing cells was desired. The valine-citrulline-*seco* duocarmycin hydroxybenzamide-azaindole (vc-*seco*-DUBA) linker-payload was selected because (i) the protease cleavable peptide linker enables bystander killing of B7-H3–negative tumor cells present in heterogeneous solid tumors, and (ii) the DNA alkylation activity of the duocarmycin payload can kill both dividing and nondividing cells, and is resistant to multidrug resistance mechanisms (28–31). The vc-*seco*-DUBA linker-payload was conjugated to MGA017 following partial reduction of the interchain disulfide bonds to generate the MGC018 ADC with an average DAR of approximately 2.7 (24). MGC018 retained the binding affinity for human and cynomolgus monkey B7-H3 observed for MGA017 (Supplementary Table S2).

In vitro profile of MGC018

MGC018-mediated *in vitro* cytotoxicity was evaluated across a set of tumor cell lines representing multiple cancer types expressing varying levels of B7-H3. MGC018 was highly potent toward all B7-H3–expressing tumor cell lines examined. A summary of the IC_{50} values for MGC018 cytotoxicity across the set of human tumor cell lines, as well as the antibody-binding capacity (ABC) and flow cytometry binding EC_{50} values of each target line, is summarized in **Table 1**.

To confirm specificity, sensitivity to MGC018 of the B7-H3–expressing cancer line, Hs700T, was compared with a derivative of the line in which B7-H3 was stably knocked out. Stable KO of B7-H3 was accomplished using B7-H3–specific CRISPR-Cas9 technology, with loss of B7-H3 cell-surface protein expression confirmed by flow cytometry (Supplementary Fig. S4). The Hs700T tumor cell line lacking B7-H3 expression (Hs700T/B7-H3 KO) was insensitive to MGC018, supporting the specificity of MGC018 toward B7-H3–expressing cancer lines (**Fig. 1A**).

Because of the nature of the cleavable vc-*seco*-DUBA linker-payload, internalization and proteolytic processing of MGC018 can lead to the release of active DUBA metabolite from dying tumor cells. The released active DUBA has the potential to be internalized by neighboring tumor cells, irrespective of B7-H3 target expression, and mediate bystander killing. To assess the potential for bystander killing, an *in vitro* coculture experiment was conducted in which Hs700T/B7-H3 KO cells, engineered to express stabilized red fluorescent protein (Hs700T/B7-H3 KO/RFP), were cultured alone, or in the presence of progressively larger amounts of unlabeled parental Hs700T cells. The cultures were incubated with MGC018 and the number of viable RFP-labeled cells (only Hs700T/B7-H3 KO/RFP cells were visible) were monitored by time-lapse fluorescent microscopy over a period of 5 days. As shown in **Fig. 1B**, treatment with MGC018 had no effect on the viability of Hs700T/B7-H3 KO/RFP cells when cultured alone (gray bar vs. white bar). Conversely, MGC018 treatment led to killing of greater than 90% of parental Hs700T cells. However, in the coculture setting, bystander killing of Hs700T/B7-H3 KO/RFP cells was observed, with the magnitude of bystander killing increasing as the

Table 1. Summary of B7-H3 expression and MGC018 *in vitro* cytotoxicity against the indicated human tumor cell lines.

Indication	Breast cancer	Melanoma	Ovarian cancer	Lung cancer		Pancreatic cancer	Glioblastoma	Colorectal cancer	B-cell lymphoma
Cancer cell line	**MDA-MB-468**	**A375.S2**	**PA-1**	**Calu-6**	**NCI-H1703**	**Hs700T**	**LN-229**	**SW48**	**Raji**
QFACS (ABC)	57,000	153,000	73,700	138,000	122,000	310,000	139,000	59,800	Negative
MGC018 flow binding EC_{50} (nmol/L)	460	456	323	406	354	797	420	253	Negative
MGC018 cytotoxicity IC_{50} (pmol/L)	767	181	275	260	585	319	910	1447	>10,000

Abbreviations: ABC, antibody-binding capacity; EC_{50}, half-maximal effective concentration; IC_{50}, half-maximal inhibitory concentration; QFACS, quantitative flow cytometry.

Downloaded from mct.aacrjournals.org on February 1, 2021. © 2020 American Association for Cancer Research.

Published OnlineFirst September 23, 2020; DOI: 10.1158/1535-7163.MCT-20-0116

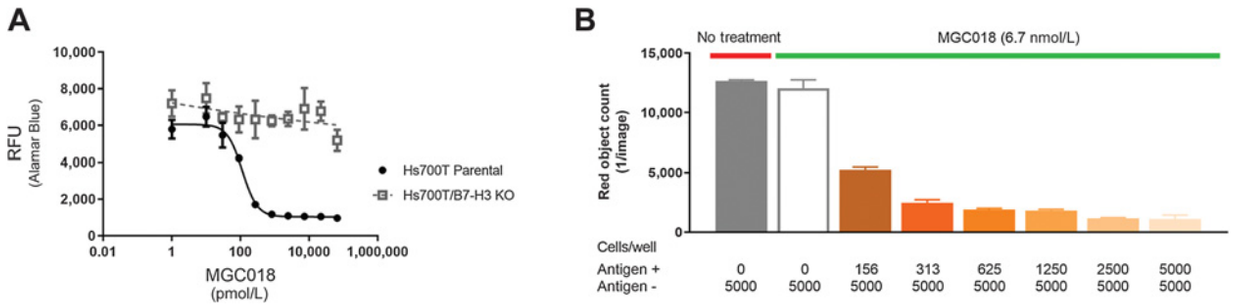

Figure 1.

MGC018 specificity and bystander activity. **A,** Evaluation of the *in vitro* cytotoxicity of MGC018 on Hs700T parental line (B7-H3 positive; closed circles) compared with a derivative of Hs700T in which B7-H3 was stably knocked out (Hs700T/B7-H3 KO; open square). Cell viability was measured by the alamarBlue cytotoxicity assay. **B,** Evaluation of bystander activity of MGC018. The indicated number of Hs700T parental cells (unlabeled, antigen positive) and Hs700T/B7-H3 KO/RFP cells (expressing red fluorescent protein, antigen negative) were mixed and incubated with 6.7 nmol/L (1 μg/mL) MGC018 or left untreated. The number of red fluorescent Hs700T/B7-H3 KO/RFP cells remaining following a 5-day incubation was counted with an IncuCyte Live-Cell Analysis System.

number of parental Hs700T cells increased (orange bars). The Supplementary Fig. S5 contains a video link of the time-lapse bystander killing. Close examination of the time-lapse microscopy revealed a temporal relationship of the bystander cytotoxicity, with killing of parental Hs700T cells commencing prior to the killing of the Hs700T/B7-H3 KO/RFP cells, consistent with payload processing and DUBA release for the bystander killing.

Serum stability and pharmacokinetics

MGC018 exhibited a high level of stability in human and cynomolgus monkey sera (Supplementary Figs. S6A and S6B). As shown in Supplementary Table S3, 111% and 85% of conjugated antibody remained following the 240-hour incubation in human or cynomolgus monkey sera, respectively. Conversely, MGC018 exhibited poor stability in wild-type CD-1 nude mouse serum. The concentration of conjugated antibody decreased rapidly following exposure to mouse serum, while the total antibody concentration remained relatively stable over the time course of exposure to serum (Supplementary Fig. S6C). Following the 240-hour incubation in mouse serum, only approximately 3% of the conjugated antibody remained. (Supplementary Table S3). The serum instability was due to the rodent-specific carboxylesterase CES1c, as MGC018 exhibited greater stability in serum from CES1c KO mice (Supplementary Fig. S6D), with approximately 65% of the conjugated antibody still remaining following the 240-hour incubation in CES1c KO mouse serum. As noted above, the instability of MGC018 in mouse serum is consistent with previous reports showing that the vc-*seco*-DUBA linker-payload is susceptible to the carboxylesterase CES1c present in rodents (24, 28).

The pharmacokinetics of MGC018 was investigated in cynomolgus monkeys following intravenous administration of MGC018 at 1, 3, 6, and 10 mg/kg. The maximum concentration (C_{max}) and total exposure (AUC_{inf}) increased with increasing dose for both total and conjugated antibody (Supplementary Fig. S7A–S7D). Consistent with the stability of MGC018 in cynomolgus serum, pharmacokinetic parameters including C_{max}, total exposure and clearance (CL) of conjugated and total antibody were similar at each dose level, and the detectable amount of unconjugated DUBA was very low (Supplementary Fig. S7A–S7D). Pharmacokinetic parameters derived from noncompartmental analysis for conjugated antibody, total antibody, and DUBA are summarized in Supplementary Tables S4–S6.

For conjugated antibody and total antibody at the dose range of 1–6 mg/kg, the mean AUC_{inf} increased more than proportionally to dose level and the drug CL decreased with increasing dose level of MGC018, suggesting a nonlinear pharmacokinetics. However, at doses above 6 mg/kg, AUC_{inf} increased proportionally to dose level and the CL was essentially unchanged. These data suggest that pharmacokinetics is linear at doses higher than 6 mg/kg, but nonlinear at the lower doses. This may be due to target-mediated drug disposition at lower doses and/or saturation of target specific CL mechanisms with increasing doses.

The pharmacokinetic properties of MGC018 following a single dose via intravenous bolus of 5 mg/kg was assessed in CD-1 nude mice, the primary species employed in the tumor xenograft studies, and in SCID/CES1c KO mice (32). Consistent with the observed instability of MGC018 in wild-type mouse serum, conjugated antibody degraded rapidly following intravenous administration of MGC018 in wild-type mice (Supplementary Fig. S7E). CL_F was considerably faster for conjugated antibody compared with total antibody (26.38 vs. 0.57 mL/hour/kg). In contrast, MGC018 exhibited favorable stability following intravenous administration in SCID/CES1c KO mice (Supplementary Fig. S7F). CL_F was very similar for conjugated antibody compared with total antibody (0.66 vs. 0.75 mL/hour/kg), respectively. Pharmacokinetic parameters derived from noncompartmental analysis for conjugated antibody and total antibody are summarized in Supplementary Table S7.

In vivo antitumor activity of MGC018

Single-dose administration

Single-dose administration of MGC018 led to a dose-dependent decrease in tumor growth of MDA-MB-468 triple-negative breast cancer xenografts (**Fig. 2A**). A rapid decrease in tumor volume was observed following treatment with MGC018 at 6 mg/kg, with a 98% reduction in tumor volume compared with the vehicle control, and 4/5 complete regressions, whereas the control ADC reduced tumor volume by 57% with no complete regressions. Treatment at 3 mg/kg with MGC018 resulted in a rapid reduction in tumor volume for 3/5 tumors, leading to 1/5 complete regressions and an overall 44% reduction in tumor volume compared with the vehicle control. Treatment at 3 mg/kg with the control ADC resulted in tumor stasis, with an overall 58% reduction in tumor volume over the course of the experiment.

Downloaded from mct.aacrjournals.org on February 1, 2021. © 2020 American Association for Cancer Research.

Published OnlineFirst September 23, 2020; DOI: 10.1158/1535-7163.MCT-20-0116

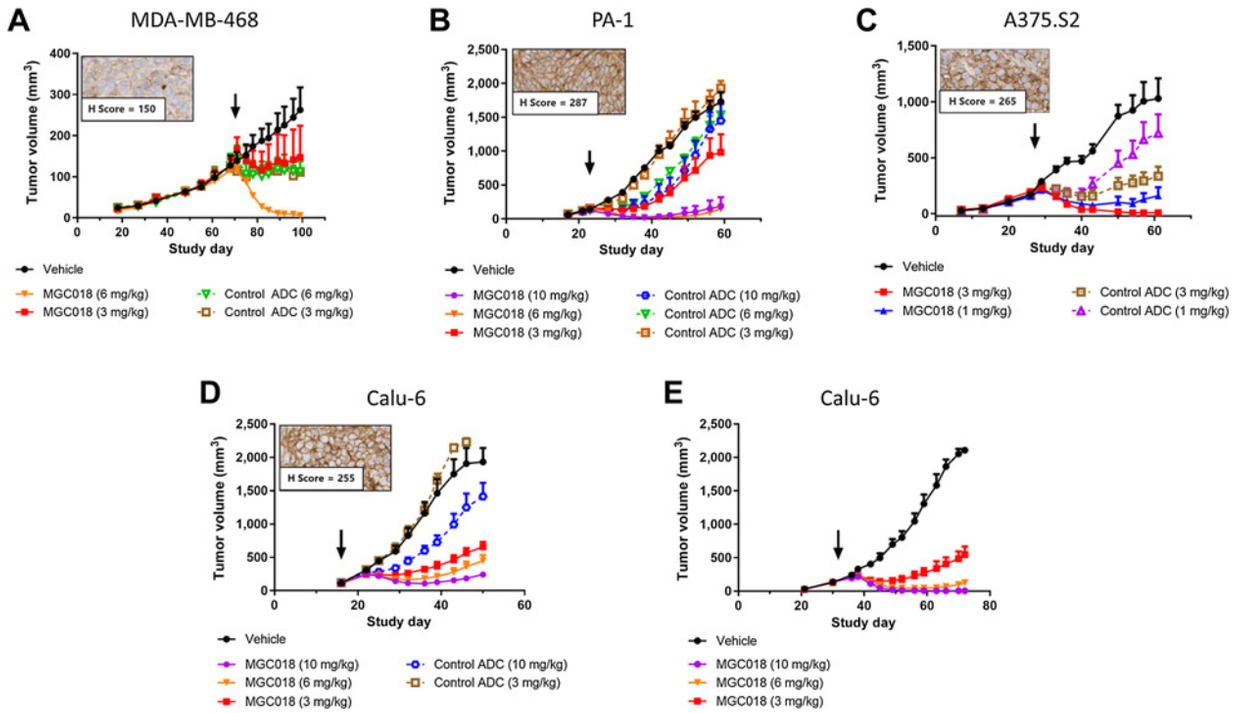

Figure 2.

MGC018 exhibits antitumor activity in multiple xenograft models. **A,** MDA-MB-468 triple-negative breast cancer orthotopic xenografts were treated with MGC018 or control ADC at 6 and 3 mg/kg. **B,** PA-1 ovarian cancer subcutaneous xenografts were treated with MGC018 or control ADC at 10, 6, and 3 mg/kg. **C,** A375.S2 melanoma subcutaneous xenografts were treated with MGC018 or control ADC at 3 and 1 mg/kg. **D,** Calu-6 lung cancer subcutaneous xenografts were treated with MGC018 or control ADC at 10, 6, and 3 mg/kg. **E,** Calu-6 lung cancer subcutaneous xenografts were treated with MGC018 ADC at 10, 6, and 3 mg/kg. Studies performed in CD-1 nude mice (**A–D**) or SCID/CES1c KO mice (**E**). Treatment day(s) are indicated by the arrows. Tumor volume is shown as group mean ± SEM. Representative images and H-scores are shown for each xenograft model.

In the PA-1 ovarian cancer xenograft, antitumor activity was observed at all three dose levels of MGC018 (**Fig. 2B**). A reduction in tumor volume of 89%, 91%, and 43%, with 3/6, 2/6, and 1/6 complete regressions, was observed following treatment with MGC018 at 10, 6, and 3 mg/kg, respectively. The control ADC exhibited minimal antitumor activity at these dose levels.

Antitumor activity was also observed against A375.S2 melanoma xenografts following a single-dose administration of MGC018 (**Fig. 2C**). At the 3 mg/kg dose level, MGC018 treatment resulted in a 99% reduction in tumor volume and 6/7 complete regressions, compared with a 67% reduction with no complete responses for the control ADC. At the 1 mg/kg dose level, MGC018 treatment resulted in an 84% reduction in tumor volume compared with a 30% reduction for the control ADC.

In a fourth model, antitumor activity was observed against Calu-6 lung cancer xenografts following administration of a single dose of MGC018 (**Fig. 2D**). A reduction in tumor volume of 91%, 84%, and 72% was observed following treatment with MGC018 at 10, 6, and 3 mg/kg, respectively. In comparison, treatment with the control ADC led to a 48% and 0% reduction in tumor volume at 10 and 3 mg/kg, respectively.

On the basis of the poor stability of MGC018 in wild-type mouse serum with ensuing limited exposure following administration in CD-1 nude mice, an *in vivo* efficacy study was conducted to assess the antitumor activity of MGC018 in SCID/CES1c KO mice. SCID/CES1c KO mice bearing Calu-6 lung cancer xenografts were administered a single dose of MGC018 or the control ADC at 10, 6, or 3 mg/kg. As shown in **Fig. 2E**, treatment with MGC018 led to a dose-dependent antitumor response, with a reduction in tumor volume of 100%, 97%, and 79% for the 10, 6, and 3 mg/kg dose, respectively, and 5/6 animals treated at 10 mg/kg had complete regressions.

Repeat-dose administration

In the clinical setting, the majority of ADCs are administered via a repeat-dose regimen, with intervals ranging from once weekly to once every 6 weeks. To evaluate the antitumor activity following repeat-dose administration, a study was performed in PA-1 ovarian cancer xenografts comparing single-dose administration to weekly times 4 (QW×4) and every other week times 4 (Q2W×4) administration. As shown in **Fig. 3A**, repeat-dose administration of MGC018 led to greater antitumor response than administration of a single dose. A single dose of 3 mg/kg MGC018 achieved short-term tumor stasis of approximately 10 days, followed by tumor regrowth. Repeat-dose administration of 3 mg/kg MGC018 led to tumor regression, resulting in a 97% and 92% reduction in tumor volume (4/6 and 2/6 complete regressions) for QW×4 and Q2W×4 treatment, respectively. The control ADC exhibited minimal antitumor activity under all dose regimens. On the basis of these results, repeat-dose administration studies (QW×4) were extended to four xenograft models with lower dose levels of MGC018.

Repeat-dose administration of MDA-MB-468 triple-negative breast cancer tumor xenografts with MGC018 resulted in a rapid decrease in tumor volume and strong overall antitumor response (**Fig. 3B**).

Downloaded from mct.aacrjournals.org on February 1, 2021. © 2020 American Association for Cancer Research.

Published OnlineFirst September 23, 2020; DOI: 10.1158/1535-7163.MCT-20-0116

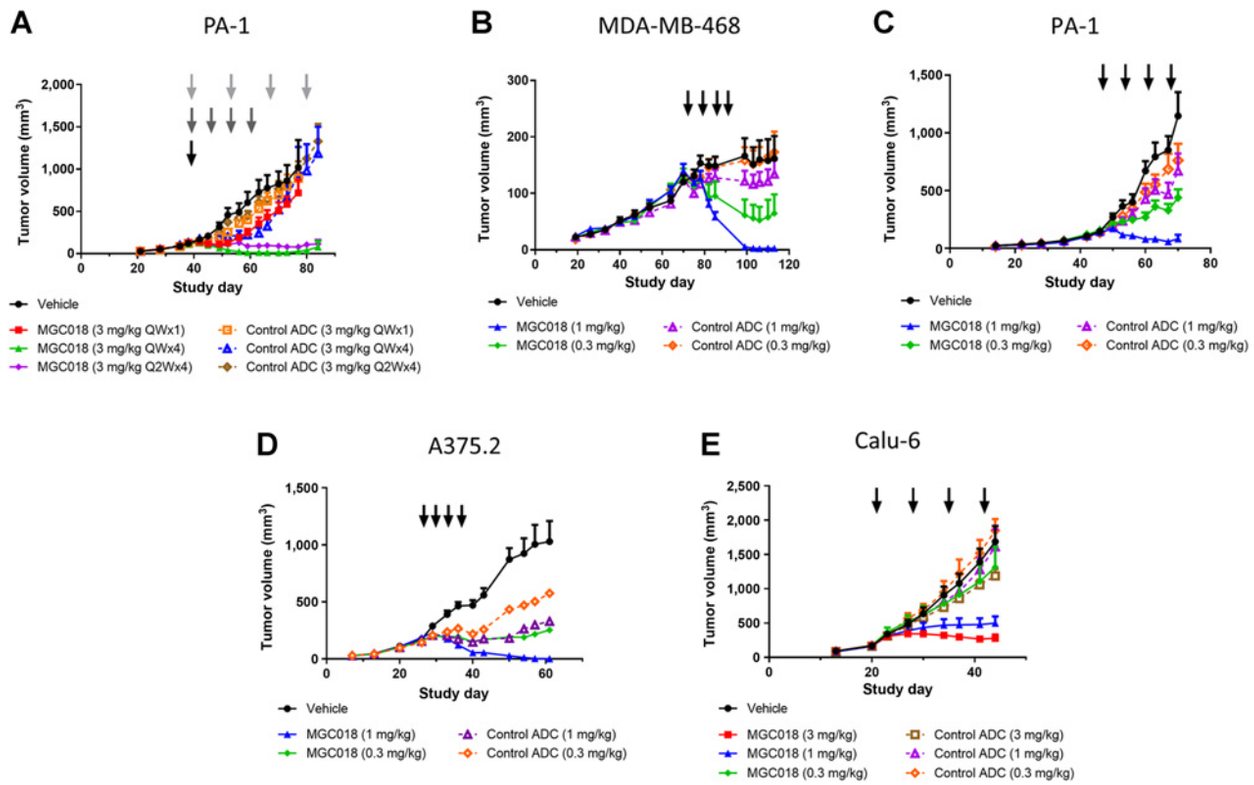

Figure 3.

MGC018 exhibits antitumor activity in multiple xenograft models following repeat-dose administration. **A,** PA-1 ovarian cancer subcutaneous xenografts were treated with MGC018 or control ADC at 3 mg/kg as a single dose (QW×1), QW×4, or Q2W×4. **B,** MDA-MB-468 triple-negative breast cancer orthotopic xenografts were treated with MGC018 or control ADC at 1 and 0.3 mg/kg QW×4. **C,** PA-1 ovarian cancer subcutaneous xenografts were treated with MGC018 or control ADC at 1 and 0.3 mg/kg QW×4. **D,** A375.S2 melanoma subcutaneous xenografts were treated with MGC018 or control ADC at 1 and 0.3 mg/kg QW×4. **E,** Calu-6 lung cancer subcutaneous xenografts were treated with MGC018 or control ADC at 3, 1, and 0.3 mg/kg QWx4. All studies were performed in CD-1 nude mice. Treatment days are indicated by the arrows. Tumor volume is shown as group mean ± SEM.

Repeat-dose administration (QW×4) resulted in a reduction in tumor volume of 98% and 60%, and complete regressions in 7/7 and 3/7 animals were observed at 1 and 0.3 mg/kg MGC018, respectively. The control ADC exhibited reduced antitumor activity compared with MGC018, with 17% and 7% reduction in tumor volume for 1 and 0.3 mg/kg, respectively. No complete regressions were observed in the control ADC treatment groups.

Dose-dependent antitumor activity was also observed toward PA-1 ovarian cancer xenografts following repeat-dose administration of MGC018 (**Fig. 3C**). Repeat-dose administration (QW×4) resulted in a reduction in tumor volume of 93% and 62% for 1 and 0.3 mg/kg MGC018, respectively. Complete regressions were observed in 2/7 animals at the 1 mg/kg MGC018. The control ADC exhibited reduced antitumor activity compared with MGC018, with 42% and 34% reduction in tumor volume for 1 and 0.3 mg/kg, respectively, with no complete regressions observed in any control ADC treatment group animals.

Antitumor activity was observed toward A375.S2 melanoma xenografts following repeat-dose administration of MGC018 at both of the doses tested (**Fig. 3D**). Repeat-dose administration (QW×4) resulted in a reduction in tumor volume of 100% and 75% for 1 and 0.3 mg/kg MGC018, respectively. Complete regressions were observed in 5/7 animals at the 1 mg/kg MGC018. The control ADC exhibited reduced antitumor activity compared with MGC018, with 68% and 44% reduction in tumor volume for 1 and 0.3 mg/kg, respectively, with one complete regression observed in the 1 mg/kg control ADC treatment group.

As shown in **Fig. 3E**, antitumor activity was also observed toward Calu-6 lung cancer xenografts following repeat-dose administration of MGC018. Repeat-dose administration (QW×4) resulted in a reduction in tumor volume of 83%, 70%, and 22% for 3, 1, and 0.3 mg/kg MGC018, respectively. Minimal activity was observed for the control ADC under the same dosing regimens.

Although antitumor activity was observed in some models with the control ADC, which is conjugated with vc-*seco*-DUBA at a similar DAR, the antitumor activity was substantially less than that observed with MGC018, consistent with target-mediated activity of MGC018. Background antitumor activity with control ADCs, including the DUBA-based control ADC employed in our studies (24, 33), has been observed by other investigators, and may result from extracellular cleavage of the linker-payload or macropinocytosis (34). To address the limitations of the control ADC, and confirm the requirement for targeting the DUBA payload to target-positive cancer cells, we conducted a study in Calu-6 lung cancer xenografts, comparing MGC018, with MGA017 (unconjugated antibody) in combination with SYD978 (free payload). In the study, we observed that MGC018 had potent antitumor activity, while the combination of MGA017 plus SYD978 had very little antitumor activity (Supplementary Fig. S8).

Downloaded from mct.aacrjournals.org on February 1, 2021. © 2020 American Association for Cancer Research.

Published OnlineFirst September 23, 2020; DOI: 10.1158/1535-7163.MCT-20-0116

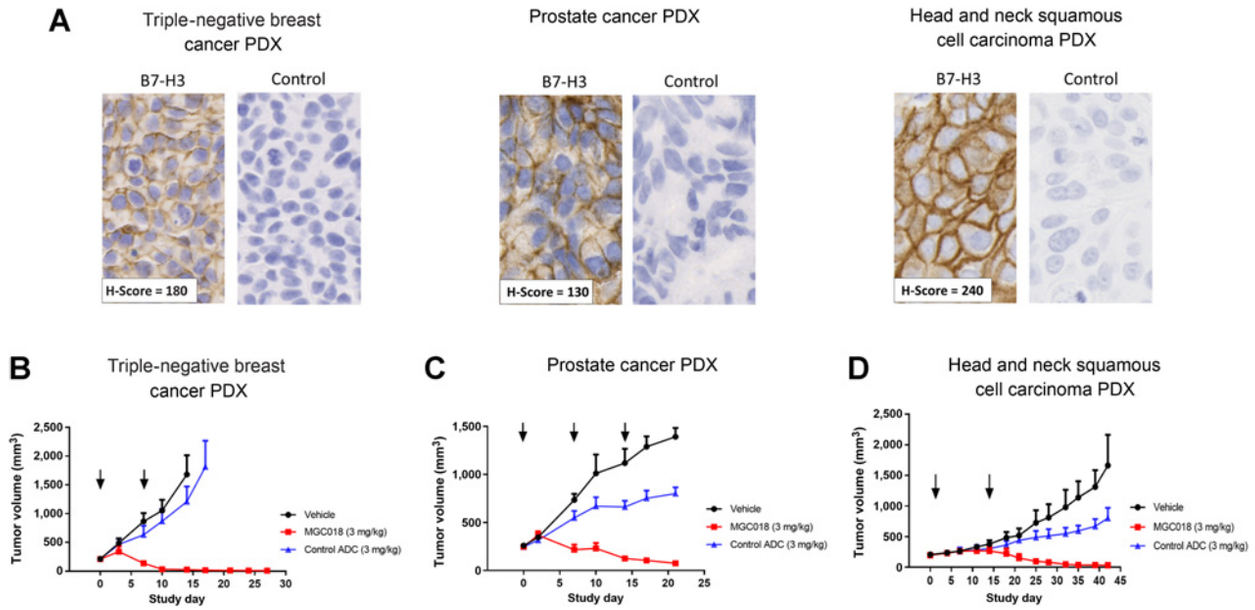

Figure 4.

MGC018 exhibits antitumor activity in multiple PDX models. **A,** representative examples of B7-H3 FFPE staining in the PDX models of triple-negative breast cancer, prostate cancer, and head and neck cancer, as well as IgG1 isotype control staining. **B,** Triple-negative breast cancer subcutaneous PDX model treated with MGC018 or control ADC at 3 mg/kg (QW×2). **C,** Prostate cancer subcutaneous PDX model treated with MGC018 or control ADC at 3 mg/kg (QW×3). **D,** Head and neck cancer subcutaneous PDX model treated with MGC018 or control ADC at 3 mg/kg (Q2W× 2). Treatment days are indicated by the arrows. Tumor volume is shown as group mean ± SEM.

PDX studies

The antitumor activity of MGC018 was also evaluated in a set of PDX models which exhibit heterogeneous expression of B7-H3 (**Fig. 4A**). Treatment of a triple-negative breast cancer PDX model (H-score 180) with MGC018 (3 mg/kg; QW×2) led to a rapid tumor regression, with a 98% reduction in tumor volume compared with the vehicle control (**Fig. 4B**). Minimal activity was observed for the control ADC. In a prostate cancer PDX model (H-score 130), rapid tumor regression, with a reduction of 95% compared with the vehicle control, was observed following treatment with MGC018 (3 mg/kg; QW×3; **Fig. 4C**). Treatment with the control ADC did not lead to tumor regression, and tumor volume was reduced by 43% compared with the vehicle control. Similarly, treatment of a squamous cell carcinoma of the head and neck PDX model (H-score 240) with MGC018 (3 mg/kg; Q2W×2) led to tumor regression and a 98% reduction in tumor volume compared with the vehicle control (**Fig. 4D**). Treatment with the control ADC did not lead to tumor regression with only 52% tumor reduction compared with the vehicle control.

MGC018 was well tolerated in all the mouse models tested. No significant weight loss or clinical signs of toxicity were observed.

Toxicology

Cynomolgus monkey was selected as a representative toxicology species for humans. The binding affinity between human and cynomolgus monkey is nearly identical for B7-H3 (K_D = 22.7 nmol/L and 22.1 nmol/L for human and cynomolgus monkey, respectively; Supplementary Table S2) and the normal tissue expression pattern of B7-H3 in cynomolgus monkey is comparable with that observed in human (13).

MGC018 administered as a 1-hour intravenous infusion every 3 weeks (total of three doses) was tolerated in cynomolgus monkeys up to 10 mg/kg/dose, the highest dose tested. All findings were minimal to mild in nature, and reversible (**Table 2**). MGC018-related clinical signs that were predominantly dose dependent included skin findings (hyperpigmentation, dry skin, erythema) and sparse hair, particularly at ≥ 6 mg/kg/dose. Slight changes in body weight gain were noted but not considered adverse.

No MGC018-related life-threatening toxicities, irreversible findings or mortality was observed in the study. MGC018-related changes in clinical pathology parameters included a mild acute inflammatory response (increases in C-reactive protein and fibrinogen), transient decreases in neutrophils, mild to moderate decrease in reticulocyte counts, decreases in lymphocytes, transient minimal to mild increases in aspartate aminotransferase (AST) and/or alanine aminotransferase (ALT) and minimal decreases in alkaline phosphatase, all of which were dose responsive in nature, reversed prior to or during the recovery phase, and did not have microscopic correlates.

On the basis of the limited and reversible nature of the findings in the study, the highest nonseverely toxic dose (HNSTD) was determined to be the highest dose administered, 10 mg/kg/dose, which corresponds to peak and systemic exposure (gender combined mean) of 310.9 μg/mL (C_{max}) and 15,075 hour*μg/mL (AUC_{inf}) for the conjugated antibody, 250.5 μg/mL (C_{max}) and 14,053 hour*μg/mL (AUC_{inf}) for the total antibody and 118.0 pg/mL (C_{max}) and 7,412 hour*pg/mL (AUC_{last}) for the free DUBA payload, respectively.

Because of the instability of MGC018 in mouse serum, rapid CL in wild-type mice, and relative stability in cynomolgus monkey, pharmacokinetic/pharmacodynamic assessments and estimates of therapeutic index are difficult to perform with confidence. The exposure of conjugated antibody in the cynomolgus monkey at the HNSTD of 10 mg/kg was 15,075 hour*μg/mL (AUC_{inf}), while the exposure in the CD-1 nude mouse was 190 hour*μg/mL (AUC_{inf}) at a dose of

Downloaded from mct.aacrjournals.org on February 1, 2021. © 2020 American Association for Cancer Research.

Published OnlineFirst September 23, 2020; DOI: 10.1158/1535-7163.MCT-20-0116

Table 2. Summary of findings in the GLP repeat-dose toxicology study in cynomolgus monkey.

Parameter	Findings
Clinical observations	• Mean body weight increased in all dose groups; however, minimal decrease in overall body weight gain at 10 mg/kg • Dose-dependent hyperpigmentation and dry skin. Erythema at locations of dry skin at ≥ 6 mg/kg. Resolved during recovery
Clinical pathology	• Transient decrease in neutrophil counts at ≥ 6 mg/kg, minimal/mild decrease in lymphocytes at 10 mg/kg. Lacked microscopic correlates, resolved during recovery • Decrease in red cell mass associated with increase in reticulocytes; less pronounced increase in reticulocytes at ≥ 6 mg/kg. Fully resolved during recovery • Increased C-reactive protein and fibrinogen. Resolved at subsequent collections • Transient minimal/mild increases in AST and/or ALT. Lacked correlative microscopic findings in the liver or muscle, resolved at subsequent collections
Gross pathology	• Skin hyperpigmentation most prominent on limbs and head at ≥ 1 mg/kg. Generally dose dependent in incidence and severity. Ongoing reversibility during recovery
Histopathology	• Skin epidermal hyperplasia, lymphocytic infiltrate, single-cell necrosis and increased pigment most prominent at ≥ 6 mg/kg. Ongoing resolution during recovery

Abbreviations: ALT, alanine aminotransferase; AST, aspartate aminotransferase.

5 mg/kg, a dose considerably higher than the efficacious dose in the repeat-dose xenograft studies in the CD-1 nude mouse. Recognizing the limitations, the preclinical data are consistent with a large therapeutic index, and provides evidence for a favorable clinical therapeutic window.

Discussion

We previously described a target-unbiased approach to generating mAbs to overexpressed cell-surface cancer antigens with therapeutic potential (35). Using this approach, we identified B7-H3 as a cell surface protein with limited expression on normal tissues but overexpressed on the epithelium and tumor-associated vasculature in solid cancers. Validation studies showed that ligation of B7-H3 by several mAbs in our panel led to mAb internalization and antitumor activity toward B7-H3–expressing tumor cells when the mAbs were conjugated to auristatin (25). On the basis of these results, we selected a lead candidate mAb and sought to develop an ADC targeting B7-H3 for the treatment of cancer.

In this article, we described the preclinical profile of MGC018, a duocarmycin-based ADC directed against B7-H3. *In vitro* studies showed that MGC018 mediated specific killing across a range of B7-H3–expressing solid tumor cell types. Owing to the hydrophobic nature of the DUBA payload, together with its conjugation via a cleavable linker, MGC018 mediated bystander killing of B7-H3–negative tumor cells in the presence of B7-H3–positive tumor cells. MGC018 exhibited potent antitumor activity in murine xenograft studies, which in general correlated with the *in vitro* cytotoxicity observed for the four models. MGC018 was active toward lung, breast, and ovarian cancer, as well as melanoma cell line–derived xenografts following a single-dose administration; furthermore, the antitumor activity was enhanced following repeat-dose administration at dose levels predicted to be achievable in the clinic based on the cynomolgus monkey toxicology profile. Importantly, MGC018 was also active toward triple-negative breast, prostate, and head and neck PDXs that exhibit heterogeneous expression of B7-H3, consistent with the bystander killing observed in coculture experiments.

In the cynomolgus monkey, MGC018 was tolerated up to 10 mg/kg/dose, the highest dose tested, when administered once every 3 weeks for a total of three doses. The toxicology profile of MGC018 was consistent with the toxicity profile reported for SYD985 (24, 36), an anti-Her2 ADC bearing the same vc-*seco*-DUBA linker-payload as MGC018, that is currently in phase III clinical testing. Several toxicities are consistent with those reported for various linker/payload platforms (i.e., transient decrease in white blood cell populations and red blood cell mass, transient increases in transaminases; refs. 37–40), but also findings such as minimal skin hyperpigmentation and epidermal hyperplasia appear to be associated with duocarmycin payloads (41). Low-level expression of both B7-H3 and Her2 has been observed in the basal layer of epithelium and sweat glands of the skin in cynomolgus monkeys; therefore, a contribution of target expression toward the skin findings cannot be ruled out. Weak expression of B7-H3 has also been observed in liver sinusoid lining cells and hepatocytes; therefore, the potential for target-mediated liver toxicity was of particular interest. Administration of MGC018 in the cynomolgus monkey led to only transient, minimal to mild increases in AST and ALT levels. While it is possible that target expression contributed to the transient increases, the AST and ALT levels remained within the historical normal range for most animals and were not associated with microscopic correlates in the liver or muscle. Neutropenia is a commonly observed toxicity with ADCs, particularly ADCs conjugated to MMAE via a cleavable valine–citrulline linker, and is proposed to represent a nontarget-mediated toxicity driven by multiple mechanisms (40, 42). As we have not observed expression of B7-H3 in neutrophils nor their precursor cells, we hypothesize that the transient decreases observed in neutrophil counts in the cynomolgus monkey following administration of MGC018 were driven by nontarget–mediated mechanisms. Other toxicities associated with tubulin modifying agents, including thrombocytopenia and peripheral sensory neuropathy, were not observed with MGC018.

The vc-*seco*-DUBA linker-payload is susceptible to the rodent-specific carboxylesterase CES1c, which leads to poor stability in wild-type mouse plasma and poor exposure in wild-type mice (24, 28, 32). As the *in vivo* efficacy of MGC018 correlates with exposure, based on dose fractionation xenograft studies, the antitumor activity of MGC018 was likely underrepresented in xenograft studies in wild-type mice. Data from our studies employing SCID/CES1c KO mice are consistent with this notion. The antitumor activity of MGC018 toward tumor xenografts in SCID/CES1c KO mice showed that greater targeted activity of MGC018 was achieved, in terms of

Downloaded from mct.aacrjournals.org on February 1, 2021. © 2020 American Association for Cancer Research.

Published OnlineFirst September 23, 2020; DOI: 10.1158/1535-7163.MCT-20-0116

reduction in tumor volume and rate of response, in the SCID/CES1c KO mice compared with wild-type CD-1 nude mice.

B7-H3 is an attractive target for cancer therapy due to its overexpression in cancer and association with disease progression and survival. We have developed two clinical-stage antibody-based therapeutics targeting B7-H3 for cancer: enoblituzumab, an Fc-optimized mAb with enhanced effector function, and MGD009, a B7-H3 × CD3 redirecting T cell DART® molecule. Interim results from an ongoing phase I study in patients with refractory B7-H3–expressing tumors and/or tumor-associated vasculature indicate enoblituzumab was well tolerated as a single agent, showed antitumor activity across several tumor types, and increased T-cell repertoire clonality in the peripheral blood of patients following treatment. The anti-B7-H3 mAb 8H9 has been investigated preclinically as both an 8H9 single-chain Fv conjugated to *Pseudomonas* exotoxin (PE38; refs. 43, 44) and as a radiolabeled mAb (10, 22, 45). ^{131}I-8H9 and ^{124}I-8H9 mAbs are currently under evaluation in pediatric central nervous system–associated cancers, where the mAbs are administered via compartmental intrathecal administration and convection-enhanced delivery (45). Beyond the published clinical studies, a B7-H3 ADC bearing an exetecan-derived payload (46), a novel afucosylated B7-H3 mAb (47) and chimeric antigen receptor T cells targeting B7-H3 (48, 49) have shown encouraging antitumor activity in preclinical studies.

Preclinical studies performed with a monomethyl-auristatin E– and pyrrolobenzodiazepine-conjugated B7-H3 ADC are particularly noteworthy (50). In several cancer types, including renal cell carcinoma and ovarian cancer, B7-H3 has been observed to be expressed not only in the tumor epithelium, but also in the tumor-associated vasculature, and provides an opportunity to target not only the tumor epithelial component, but also the tumor-associated stroma. Indeed, Seaman and colleagues (50) showed that an anti-B7-H3 ADC can destroy both the tumor epithelium and tumor vasculature, eradicating established tumors and metastasis, resulting in improved long-term overall survival. Importantly, this study showed that sensitivity of the tumor vasculature was dependent on the nature of the payload. While a pyrrolobenzodiazepine-conjugated ADC was effective at killing both tumor epithelium and tumor-associated vasculature, the auristatin-conjugated ADC was only effective in killing tumor epithelium. The resistance of tumor-associated vasculature to the auristatin-conjugated ADC was linked in part to expression of the ATP-binding cassette transporter P-glycoprotein. In addition, differences in the growth rate of tumor epithelium compared with tumor-associated vasculature may contribute to resistance to tubulin-modifying agents, since those agents are only cytotoxic to actively dividing cells. Although we were unable to test MGC018 in this context due to its lack of cross-reactivity with mouse B7-H3, duocarmycin is a DNA damaging agent that is cytotoxic toward both dividing and nondividing tumor cells and would be anticipated to be cytotoxic toward both tumor epithelium and tumor-associated vasculature. Furthermore, duocarmycin is also a poor substrate for P-glycoprotein (28, 29).

In conclusion, we have developed an anti-B7-H3 ADC, MGC018, that incorporates a duocarmycin-based DNA alkylating payload via a cleavable valine–citrulline linker. MGC018 exhibits potent antitumor activity across a range of human tumor xenografts, mediates bystander killing and shows a favorable safety profile in cynomolgus monkey. The antitumor activity observed preclinically with MGC018, together with the positive safety profile, provides evidence of a potentially favorable therapeutic index and supports the continued development of MGC018 for the treatment of solid cancers.

Disclosure of Potential Conflicts of Interest

All authors report Byondis B.V. (formerly Synthon Biopharmaceuticals B.V.) has licensed rights to its linker-drug technology to MacroGenics, Inc. to enable development and commercialization of MGC018. Byondis B.V. provides manufacturing support and supplies the conjugated MGC018 to MacroGenics Inc., Byondis B.V. will be entitled to receive license fees, milestone payments and royalties based on successful development and commercialization of MGC018.

Authors' Contributions

J.A. Scribner: Conceptualization, formal analysis, supervision, investigation, methodology, writing-original draft, writing-review and editing. **J.G. Brown:** Conceptualization, formal analysis, supervision, methodology, writing-original draft. **T. Son:** Investigation, methodology, writing-original draft. **M. Chiechi:** Investigation, methodology. **P. Li:** Investigation. **S. Sharma:** Formal analysis, methodology. **H. Li:** Formal analysis, supervision, investigation, methodology. **A. De Costa:** Investigation, methodology. **Y. Li:** Investigation, methodology. **Y. Chen:** Investigation, methodology. **A. Easton:** Investigation, methodology. **N.C. Yee-Toy:** Investigation, methodology. **F.Z. Chen:** Formal analysis, supervision, methodology. **S. Gorlatov:** Investigation, methodology. **B. Barat:** Investigation, methodology. **L. Huang:** Investigation, methodology. **C.R. Wolff:** Investigation, methodology. **J. Hooley:** Investigation, methodology, writing-original draft. **T.E. Hotaling:** Investigation, methodology. **T. Gaynutdinov:** Investigation, methodology. **V. Ciccarone:** Supervision, investigation, methodology. **J. Tamura:** Formal analysis, supervision, investigation, methodology. **S. Koenig:** Conceptualization, supervision, writing-review and editing. **P.A. Moore:** Conceptualization, supervision, writing-review and editing. **E. Bonvini:** Conceptualization, supervision, writing-original draft, writing-review and editing. **D. Loo:** Conceptualization, supervision, methodology, writing-original draft, writing-review and editing.

Acknowledgments

The authors thank the following people for their invaluable contributions: Neely Gal-Edd for project management, Kathleen Shiffer and Melinda Hanson for lab management, and Judy Downey for editorial assistance. The DUBA linker-payload was provided and conjugated by Byondis B.V. Finally, we would like to pay our respects and acknowledge the wide-ranging contributions of Syd Johnson toward the work presented in this manuscript. Syd Johnson passed away in December 2018.

The costs of publication of this article were defrayed in part by the payment of page charges. This article must therefore be hereby marked *advertisement* in accordance with 18 U.S.C. Section 1734 solely to indicate this fact.

Received February 14, 2020; revised June 2, 2020; accepted September 15, 2020; published first September 23, 2020.

References

1. Zang X, Allison JP. The B7 family and cancer therapy: costimulation and coinhibition. Clin Cancer Res 2007;13:5271–9.
2. Ling V, Wu PW, Spaulding V, Kieleczawa J, Luxenberg D, Carreno BM, et al. Duplication of primate and rodent B7-H3 immunoglobulin V- and C-like domains: divergent history of functional redundancy and exon loss. Genomics 2003;82:365–77.
3. Steinberger P, Majdic O, Derdak SV, Pfistershammer K, Kirchberger S, Klauser C, et al. Molecular characterization of human 4Ig-B7-H3, a member of the B7 family with four Ig-like domains. J Immunol; 2004; 172:2352–9.
4. Hofmeyer KA, Ray A, Zang X. The contrasting role of B7-H3. Proc Natl Acad Sci U S A 2008;105:10277–8.
5. Pardoll DM. The blockade of immune checkpoints in cancer immunotherapy. Nat Rev Cancer 2012;12:252–64.
6. Prasad DV, Nguyen T, Li Z, Yang Y, Duong J, Wang Y, et al. Murine B7-H3 is a negative regulator of T cells. J Immunol 2004;173:2500–6.

Downloaded from mct.aacrjournals.org on February 1, 2021. © 2020 American Association for Cancer Research.

Published OnlineFirst September 23, 2020; DOI: 10.1158/1535-7163.MCT-20-0116

7. Suh WK, Gajewska BU, Okada H, Gronski MA, Bertram EM, Dawicki W, et al. The B7 family member B7-H3 preferentially down-regulates T helper type 1-mediated immune responses. Nat Immunol 2003;4:899–906.
8. Wang L, Fraser CC, Kikly K, Wells AD, Han R, Coyle AJ, et al. B7-H3 promotes acute and chronic allograft rejection. Eur J Immunol 2005;35:428–38.
9. Vigdorovich V, Ramagopal UA, Lazar-Molnar E, Sylvestre E, Lee JS, Hofmeyer KA, et al. Structure and T cell inhibition properties of B7 family member, B7–H3. Structure 2013;21:707–17.
10. Ahmed M, Cheng M, Zhao Q, Goldgur Y, Cheal SM, Guo HF, et al. Humanized affinity-matured monoclonal antibody 8H9 has potent antitumor activity and binds to FG loop of tumor antigen B7-H3. J Biol Chem 2015;290:30018–29.
11. Zang X, Thompson RH, Al-Ahmadie HA, Serio AM, Reuter VE, Eastham JA, et al. B7-H3 and B7x are highly expressed in human prostate cancer and associated with disease spread and poor outcome. Proc Natl Acad Sci U S A 2007;104:19458–63.
12. Chavin G, Sheinin Y, Crispen PL, Boorjian SA, Roth TJ, Rangel L, et al. Expression of immunosuppresive B7-H3 ligand by hormone-treated prostate cancer tumors and metastases. Clin Cancer Res 2009;15:2174–80.
13. Loo D, Alderson RF, Chen FZ, Huang L, Zhang W, Gorlatov S, et al. Development of an Fc-enhanced anti-B7-H3 monoclonal antibody with potent antitumor activity. Clin Cancer Res 2012;18:3834–45.
14. Roth TJ, Sheinin Y, Lohse CM, Kuntz SM, Frigola X, Inman BA, et al. B7-H3 ligand expression by prostate cancer: a novel marker of prognosis and potential target for therapy. Cancer Res 2007;67:7893–900.
15. Wang J, Chong KK, Nakamura Y, Nguyen L, Huang SK, Kuo C, et al. B7-H3 associated with tumor progression and epigenetic regulatory activity in cutaneous melanoma. J Invest Dermatol 2013;133:2050–8.
16. Liu C, Liu J, Wang J, Liu Y, Zhang F, Lin W, et al. B7-H3 expression in ductal and lobular breast cancer and its association with IL-10. Mol Med Rep 2013;7:134–8.
17. Maeda N, Yoshimura K, Yamamoto S, Kuramasu A, Inoue M, Suzuki N, et al. Expression of B7-H3, a potential factor of tumor immune evasion in combination with the number of regulatory T cells, affects against recurrence-free survival in breast cancer patients. Ann Surg Oncol 2014;21:S546–54.
18. Sun Y, Wang Y, Zhao J, Gu M, Giscombe R, Lefvert AK, et al. B7-H3 and B7-H4 expression in non-small-cell lung cancer. Lung Cancer 2006;53:143–51.
19. Mao Y, Li W, Chen K, Xie Y, Liu Q, Yao M, et al. B7-H1 and B7-H3 are independent predictors of poor prognosis in patients with non-small cell lung cancer. Oncotarget 2015;6:3452–61.
20. Chen JT, Chen CH, Ku KL, Hsiao M, Chiang CP, Hsu TL, et al. Glycoprotein B7-H3 overexpression and aberrant glycosylation in oral cancer and immune response. Proc Natl Acad Sci U S A 2015;112:13057–62.
21. Crispen PL, Sheinin Y, Roth TJ, Lohse CM, Kuntz SM, Frigola X, et al. Tumor cell and tumor vasculature expression of B7-H3 predict survival in clear cell renal cell carcinoma. Clin Cancer Res 2008;14:5150–7.
22. Modak S, Kramer K, Gultekin SH, Guo HF, Cheung NK. Monoclonal antibody 8H9 targets a novel cell surface antigen expressed by a wide spectrum of human solid tumors. Cancer Res 2001;61:4048–54.
23. Xu H, Cheung IY, Guo HF, Cheung NK. MicroRNA miR-29 modulates expression of immunoinhibitory molecule B7-H3: potential implications for immune based therapy of human solid tumors. Cancer Res 2009;69:6275–81.
24. Dokter W, Ubink R, van der Lee M, van der Vleuten M, van Achterberg T, Jacobs D, et al. Preclinical profile of the HER2-targeting ADC SYD983/SYD985: introduction of a new duocarmycin-based linker-drug platform. Mol Cancer Ther 2014;13:2618–29.
25. Loo D, Scribner J, Son T, Hooley J, Hotaling T, Chiechi M, et al. Anti-B7-H3 antibody-drug conjugates as potential therapeutics for solid cancer [abstract]. In: Proceedings of the 107th Annual Meeting of the American Association for Cancer Research; 2016 Apr 16–20; New Orleans, LA. Philadelphia (PA): AACR; Cancer Res 2016;76(14 Suppl):Abstract nr 1201.
26. Zang X, Sullivan PS, Soslow RA, Waitz R, Reuter VE, Wilton A, et al. Tumor associated endothelial expression of B7-H3 predicts survival in ovarian carcinomas. Mod Pathol 2010;23:1104–12.
27. Bin Z, Guangbo Z, Yan G, Huan Z, Desheng L, Xueguang Z. Overexpression of B7-H3 in CD133+ colorectal cancer cells is associated with cancer progression and survival in human patients. J Surg Res 2014;188:396–403.
28. Elgersma RC, Coumans RG, Huijbregts T, Menge WM, Joosten JA, Spijker HJ, et al. Design, synthesis, and evaluation of linker-duocarmycin payloads: toward selection of HER2-targeting antibody-drug conjugate SYD985. Mol Pharm 2015;12:1813–35.
29. Giddens AC, Lee HH, Lu GL, Miller CK, Guo J, Lewis Phillips GD, et al. Analogues of DNA minor groove cross-linking agents incorporating aminoCBI, an amino derivative of the duocarmycins: synthesis, cytotoxicity, and potential as payloads for antibody-drug conjugates. Bioorg Med Chem 2016;24:6075–81.
30. Kobayashi E, Okamoto A, Asada M, Okabe M, Nagamura S, Asai A, et al. Characteristics of antitumor activity of KW-2189, a novel water-soluble derivative of duocarmycin, against murine and human tumors. Cancer Res 1994;54:2404–10.
31. Gomi K, Kobayashi E, Miyoshi K, Ashizawa T, Okamoto A, Ogawa T, et al. Anticellular and antitumor activity of duocarmycins, novel antitumor antibiotics. Jpn J Cancer Res 1992;83:113–20.
32. Ubink R, Dirksen EHC, Rouwette M, Bos ES, Janssen I, Egging DF, et al. Unraveling the interaction between carboxylesterase 1c and the antibody-drug conjugate SYD985: improved translational PK/PD by using ces1c knockout mice. Mol Cancer Ther 2018;17:2389–98.
33. van der Lee MM, Groothuis PG, Ubink R, van der Vleuten MA, van Achterberg TA, Loosveld EM, et al. The preclinical profile of the duocarmycin-based HER2-targeting ADC SYD985 predicts for clinical benefit in low HER2-expressing breast cancers. Mol Cancer Ther 2015;14:692–703.
34. Ha KD, Bidlingmaier SM, Liu B. Macropinocytosis exploitation by cancers and cancer therapeutics. Front Physiol 2016;7:381.
35. Loo DT, Mather JP. Antibody-based identification of cell surface antigens: targets for cancer therapy. Curr Opin Pharmacol 2008;8:627–31.
36. Banerji U, van Herpen CML, Saura C, Thistlethwaite F, Lord S, Moreno V, et al. Trastuzumab duocarmazine in locally advanced and metastatic solid tumours and HER2-expressing breast cancer: a phase 1 dose-escalation and dose-expansion study. Lancet Oncol 2019;20:1124–35.
37. Hinrichs MJ, Dixit R. Antibody drug conjugates: nonclinical safety considerations. AAPS J 2015;17:1055–64.
38. Masters JC, Nickens DJ, Xuan D, Shazer RL, Amantea M. Clinical toxicity of antibody drug conjugates: a meta-analysis of payloads. Invest New Drugs 2018;36:121–35.
39. Saber H, Leighton JK. An FDA oncology analysis of antibody-drug conjugates. Regul Toxicol Pharmacol 2015;71:444–52.
40. Donaghy H. Effects of antibody, drug and linker on the preclinical and clinical toxicities of antibody-drug conjugates. MAbs 2016;8:659–71.
41. Owonikoko TK, Hussain A, Stadler WM, Smith DC, Kluger H, Molina AM, et al. First-in-human multicenter phase I study of BMS-936561 (MDX-1203), an antibody-drug conjugate targeting CD70. Cancer Chemother Pharmacol 2016;77:155–62.
42. Zhao H, Gulesserian S, Malinao MC, Ganesan SK, Song J, Chang MS, et al. A potential mechanism for ADC-induced neutropenia: role of neutrophils in their own demise. Mol Cancer Ther 2017;16:1866–76.
43. Onda M, Wang QC, Guo HF, Cheung NK, Pastan I. *In vitro* and *in vivo* cytotoxic activities of recombinant immunotoxin 8H9(Fv)-PE38 against breast cancer, osteosarcoma, and neuroblastoma. Cancer Res 2004;64:1419–24.
44. Luther N, Cheung NK, Souliopoulos EP, Karampelas I, Bassiri D, Edgar MA, et al. Interstitial infusion of glioma-targeted recombinant immunotoxin 8H9scFv-PE38. Mol Cancer Ther 2010;9:1039–46.
45. Kramer K, Kushner BH, Modak S, Pandit-Taskar N, Smith-Jones P, Zanzonico P, et al. Compartmental intrathecal radioimmunotherapy: results for treatment for metastatic CNS neuroblastoma. J Neurooncol 2010;97:409–18.
46. Ogitani Y, Abe Y, Iguchi T, Yamaguchi J, Terauchi T, Kitamura M, et al. Wide application of a novel topoisomerase I inhibitor-based drug conjugation technology. Bioorg Med Chem Lett 2016;26:5069–72.
47. Nagase-Zembutsu A, Hirotani K, Yamato M, Yamaguchi J, Takata T, Yoshida M, et al. Development of DS-5573a: a novel afucosylated mAb directed at B7-H3 with potent antitumor activity. Cancer Sci 2016;107:674–81.
48. Du H, Hirabayashi K, Ahn S, Kren NP, Montgomery SA, Wang X, et al. Antitumor responses in the absence of toxicity in solid tumors by targeting B7-H3 via chimeric antigen receptor T cells. Cancer Cell 2019;35:221–37 e8.
49. Majzner RG, Theruvath JL, Nellan A, Heitzeneder S, Cui Y, Mount CW, et al. CAR T cells targeting B7-H3, a pan-cancer antigen, demonstrate potent preclinical activity against pediatric solid tumors and brain tumors. Clin Cancer Res 2019;25:2560–74.
50. Seaman S, Zhu Z, Saha S, Zhang XM, Yang MY, Hilton MB, et al. Eradication of tumors through simultaneous ablation of CD276/B7-H3-positive tumor cells and tumor vasculature. Cancer Cell 2017;31:501–15 e8.

Downloaded from mct.aacrjournals.org on February 1, 2021. © 2020 American Association for Cancer Research.

Published OnlineFirst September 23, 2020; DOI: 10.1158/1535-7163.MCT-20-0116

AACR American Association for Cancer Research

Molecular Cancer Therapeutics

Preclinical Development of MGC018, a Duocarmycin-based Antibody–drug Conjugate Targeting B7-H3 for Solid Cancer

Juniper A. Scribner, Jennifer G. Brown, Thomas Son, et al.

Mol Cancer Ther 2020;19:2235-2244. Published OnlineFirst September 23, 2020.

Updated version Access the most recent version of this article at: doi:10.1158/1535-7163.MCT-20-0116

Supplementary Material Access the most recent supplemental material at: http://mct.aacrjournals.org/content/suppl/2020/09/24/1535-7163.MCT-20-0116.DC1

Visual Overview **A diagrammatic summary of the major findings and biological implications:** http://mct.aacrjournals.org/content/19/11/2235/F1.large.jpg

Cited articles This article cites 48 articles, 20 of which you can access for free at: http://mct.aacrjournals.org/content/19/11/2235.full#ref-list-1

E-mail alerts Sign up to receive free email-alerts related to this article or journal.

Reprints and Subscriptions To order reprints of this article or to subscribe to the journal, contact the AACR Publications Department at pubs@aacr.org.

Permissions To request permission to re-use all or part of this article, use this link http://mct.aacrjournals.org/content/19/11/2235. Click on "Request Permissions" which will take you to the Copyright Clearance Center's (CCC) Rightslink site.

Downloaded from mct.aacrjournals.org on February 1, 2021. © 2020 American Association for Cancer Research.